Entropy and heat capacity calculations of simulated crystal–hexatic smectic-*B*–smectic-*A* liquid-crystal phase transitions

Keiko M. Aoki,* Makoto Yoneya, and Hiroshi Yokoyama

Yokoyama Nanosystem Liquid Crystal Project, JST, Tsukuba, Japan

Entropy and heat capacity are calculated in phase sequence of crystal, hexatic smectic-*B*, and smectic-*A* liquid crystals through constant pressure and temperature molecular-dynamics simulations of parallel soft spherocylinders. The transition from crystal to hexatic smectic-*B* phase is continuous while the transition to smectic-*A* phase is first order. The dependence of the phase sequence against the molecular shape anisotropy is investigated and there exists a triple point at a rather small anisotropy. Hopping diffusion of molecules is observed in the hexatic smectic-*B* phase.

Entropy S is a fundamental quantity in physics. In molecular simulations, S has been estimated through statistical physics approach [1] calculating $S = -k_B \Sigma p^B \ln p^B$. The value of Boltzmann probability p^B depends not only on each configuration but also on the entire ensemble through the partition function, thus the quality of sampling is always crucial. A different approach to calculate S through the absorption or production of heat in the system, i.e., thermodynamic approach, has been proposed recently [2]. Precise calculation of the change in heat is possible by this method due to the structure of the Hamiltonian.

Phases with hexatic order, characterized by quasi-long-range sixfold bond orientational order (BOO), have been extensively studied in smectic phases (which are stacks of liquid layers) of liquid crystal compounds [3] and are relevant to many other systems including superfluids, superconductors, and liquid membrane to mention a few. Despite of the work accumulated to date, many aspects remain to be clarified in relation to the theory of defect-mediated melting transition [4]. The hexatic smectic-*B* (Hex*B*) phase can be considered as consisting of stacked two-dimensional (2D) hexatic layers, however, the correlations between the layers are also very important since three-dimensional (3D) sixfold BOOs are observed in these systems. The effect of the most basic characteristic of liquid crystal materials, i.e., anisotropy of the molecular shape, is investigated in systems of hardcore spherocylinders [5] as well as soft spherocylinders with rotation [6]. However, in neither of these systems the Hex*B* phase appears. By hindering the rotation of the long axis of soft spherocylinders, it has been shown that excluded volume effect alone can give rise to the Hex*B* phase [7], however due to the limitation of the simulation methods, the investigation was quite limited. The system of parallel soft spherocylinders is the most primitive model to give rise to the Hex*B* phase which is consistent with the fact that the orientational order of the long molecular axis is generally very high in Hex*B* phase.

By thermodynamic approach, the relative entropy and heat capacity are calculated through the phase sequence of crystal (Cry), Hex*B*, and smectic *A* (Sm*A*) and are used to

define the phase-transition temperatures. We obtain a phase diagram under constant pressure and temperature. In the Sm*A* phase, no BOO exists. Not only the nature of the first-order transition of Hex*B*-Sm*A* but also the continuous nature of Cry-Hex*B* phase transition is clearly identified. In former studies, the identification of the Cry-Hex*B* phase-transition boundaries has been done through analysis of bond orientational correlation functions [8] or dual criterion of molecular hopping rate and bond order [9]. We also show that dynamical heterogeneity usually discussed in the context of metastable states, such as glass or supercooled liquid [10], also appears in Hex*B* phase.

The model particles are parallel soft spherocylinders resembling that of Kihara [11] which express the interaction between anisotropic molecules through minimum distance between them. However, instead of using interaction with both repulsive and attractive parts, we use purely repulsive pairwise potential (just as Weeks *et al.* potential [12] is the purely repulsive part of the Lennard-Jones potential)

$$\phi_{ij} = \begin{cases} \epsilon \left\{ \left(\dfrac{D}{R_{ij}}\right)^{12} - \left(\dfrac{D}{R_{ij}}\right)^6 + \dfrac{1}{4} \right\} & \text{if } R_{ij} < r_0 \\ 0 & \text{otherwise,} \end{cases} \quad (1)$$

where $r_0 = 2^{1/6}D$ and R_{ij} is the shortest distance between lines (where the potential is infinite) representing the long axis of the two spherocylinders, i.e.,

$$R_{ij}^2 = \begin{cases} x_{ij}^2 + y_{ij}^2 & \text{if } |z_{ij}| \le L \\ x_{ij}^2 + y_{ij}^2 + (|z_{ij}| < L)^2 & \text{otherwise,} \end{cases} \quad (2)$$

where (x_{ij}, y_{ij}, z_{ij}) is the relative position of the center of mass of the spherocylinders i and j, and L is the length of the line representing the long axis of the spherocylinder which is fixed parallel to the z axis. This corresponds to taking the moment of inertia as infinite. Translation of the spherocylinders is free. Periodic boundary conditions are applied in x, y, and z directions. Reduced units where length, energy, and mass are measured in D, ϵ, and m (where m is the mass of a spherocylinder), respectively, are used throughout this work. We mainly report results for systems with number of spherocylinders $N = 1344$ which form six layers. Calculations with $N = 1170$, 2340, 4680, and 9360 were also conducted to
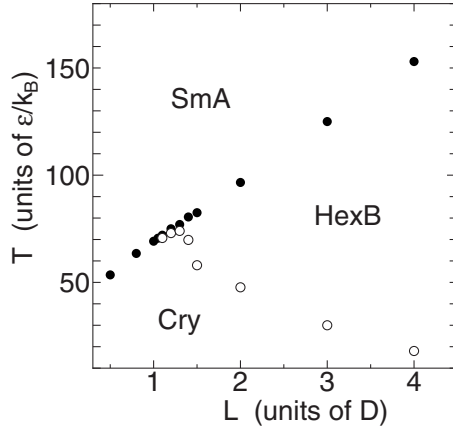
---

*aoki@icfd.co.jp

FIG. 1. Phase diagram of $N=1344$ parallel soft spherocylinders at $P=1000$ for various lengths L. Transition temperatures are identified from function $(1-\nu)/T$ consisting the relative entropy for Cry-Hex$B$ phase transition (○) and transition to SmA phase (●).

check the system size effects. Time step of calculation is $\delta t = 1.0 \times 10^{-4}$ for all the runs. Data for different temperatures are obtained by independent runs starting from identical initial configurations for each L. Each data is an average value for time duration $\Delta t=100$ (i.e., 1×10^6 time steps) at the end of $t \geq 1100$ calculation unless otherwise stated. The masses of the barostat and thermostat are, respectively, $M=0.01$ and $K=20\,000$ for most of the calculations.

The molecular-dynamics (MD) method we use was designed to simulate soft matter effectively [2] by using an explicit symplectic integrator [13]. The barostat is designed to conform to the changes in both shape and bulk elasticities by effectively dealing the anisotropic fluctuations [14]. The thermostat is a Hamiltonian version of Nosé-Hoover dynamics [15]. The entropy is calculated from the change in heat ΔQ, i.e.,

$$\Delta S = \frac{\Delta Q}{T} = \frac{1-\nu}{T}(-W), \qquad (3)$$

where ν is the time scaling factor of the Poincaré time transformation and W is the work [2]. Especially the function $(1-\nu)/T$ is useful in identifying the nature of the phase transition, since W is a monotonically slow varying function quite small compared to the value of the original Hamiltonian itself. The change in the value of ν (initially set to $\nu=1$) is reflecting the absorption or production of heat in the system.

Phase diagram under constant pressure $P=1000$ of parallel spherocylinders with various lengths L is given in Fig. 1. Triple point of Cry, Hex$B$, and SmA phases appears at $1.0 < L < 1.05$. This length is close to the value where Hex$B$ phase has been previously reported [7]. As the length of the spherocylinder gets longer, Cry-Hex$B$ transition temperature T_{CB} decreases. This tendency coincides with that of crystal-hexatic transition temperature of membranes confined in two parallel plates (see Fig. 1.6 in [4]). The transition temperature to SmA phase (independent whether it is from Cry or Hex$B$ phase) is linearly dependent on the molecular length L. The linear dependence of crystal-smectic phase-transition
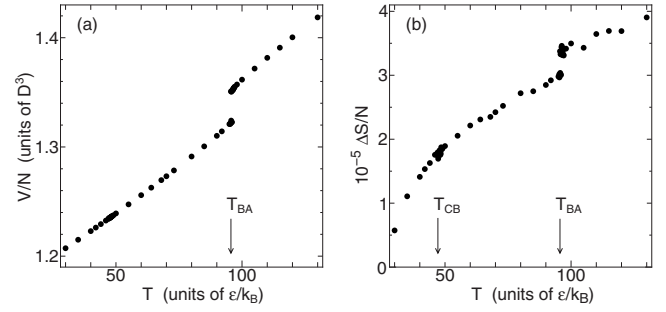
temperature on molecular length has also been observed in soft parallel spherocylinders interacting via inverse power potential [16].

In Fig. 2, partial molar (a) volume V/N and (b) relative entropy $\Delta S/N$ [2] against temperature T are shown for systems of $L=2$. Partial molar volume $\bar{v}=V/N$ and entropy $\bar{s}=S/N$ along with internal energy $\bar{u}=U/N$ are related to the partial molar Gibbs free energy $\partial G/\partial N$, i.e., the chemical potential μ, through $(\partial G/\partial N)_{P,T}=\mu=\bar{u}+\bar{v}P-\bar{s}T$. Figure 2 shows that V/N and $\Delta S/N$ only jump at the Hex$B$-SmA transition temperature T_{BA}. However, the partial molar relative entropy $\Delta S/N$ [Fig. 2(b)] has a kink at T_{CB} and clearly shows the continuous nature of this transition. Since the chemical potential must be continuous at the Hex$B$-SmA phase transition, the enthalpy and entropy must compensate [17] at T_{BA}, i.e., $\delta\bar{u}|_{BA}+\delta\bar{v}|_{BA}P=\delta\bar{s}|_{BA}T_{BA}$, where $\delta\bar{u}|_{BA}$, $\delta\bar{v}|_{BA}$, and $\delta\bar{s}|_{BA}$ are, respectively, the jump in values of $\bar{u}$, $\bar{v}$, and $\bar{s}$ at the transition. By using this relation to obtain $\delta\bar{s}|_{BA}$ and comparing it to the jump in the value of $\Delta S/N$ at T_{BA}, the difference in scale (in simulation units) of the relative entropy ΔS and true entropy S is known at T_{BA}. Extrapolation of $\Delta S/N$ to zero is at $T \simeq 28$ for Fig. 2(b), since the initial configuration used for the series of calculation for $L=2$ is that of $T=28$. Volumetric studies by experiments are rare, however, the only study we are aware of for Crys-Hex$B$-SmA phase sequence [18] shows resemblance to Fig. 2(a).

In Fig. 3, we further divide the relative partial molar entropy plotted in Fig. 2(b) into two terms, $(1-\nu)/T$ and $-W$. It

FIG. 2. Partial molar (a) volume and (b) relative entropy for $N=1344$ parallel soft spherocylinders with $L=2$ at $P=1000$.
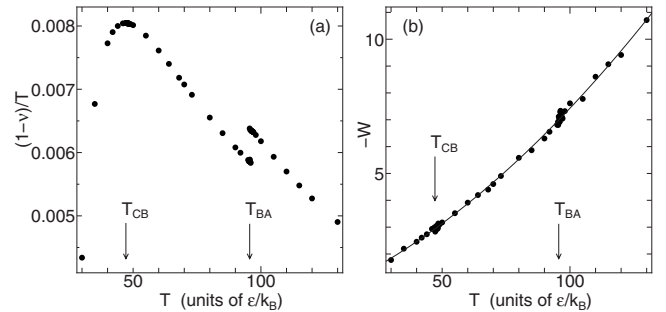

FIG. 3. Functions (a) $(1-\nu)/T$ and (b) $-W$ consisting the partial molar relative entropy $\Delta S/N$ in Fig. 2(b) for $N=1344$ parallel soft spherocylinders with $L=2$ at $P=1000$. The line in (b) is the fitted temperature dependence $-W(T)=3.549 \times 10^{-1}+4.055 \times 10^{-2}T +3.018 \times 10^{-4}T^2$. Value of initial Hamiltonian is $\mathcal{H}_0=1.942341 \times 10^6$ for this series of calculation.
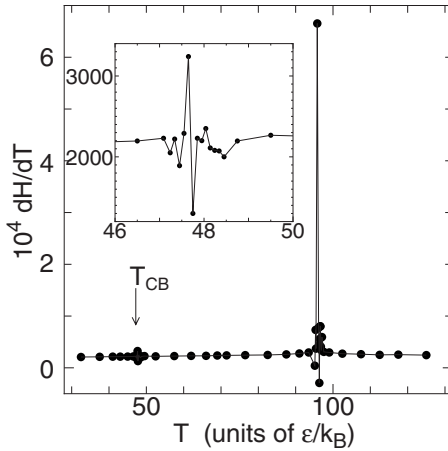
FIG. 4. Temperature dependence of dH/dT for $N=1344$ parallel soft spherocylinders with $L=2$ at $P=1000$.

is evident that the $(1-\nu)/T$ term [Fig. 3(a)] shows the characteristics of the phase transitions clearly, i.e., the continuous nature at T_{CB} and the first-order nature at T_{BA}. Especially, the usefulness of function $(1-\nu)/T$ to determine T_{CB} is clearly demonstrated since there exists an extremum at T_{CB} whereas there is only a kink in the entropy curve. In the case of spherical soft particles, the function $(1-\nu)/T$ has been almost proportional to the $\Delta S/N$ curve near the crystal-isotropic liquid phase transition [2]. For shorter parallel spherocylinders where crystal melts directly to SmA phase ($L \leq 1$), we observed a similar behavior in $(1-\nu)/T$.

The differential dH/dT of enthalpy with respect to temperature is shown in Fig. 4. This quantity corresponds to the curve obtained by differential scanning calorimetry (DSC) in experiments. However, the thermodynamic properties reported here are free from effects of cooling or heating rates since independently equilibrated calculations are conducted at each temperature.

Figure 5 shows the molar heat capacity C_P calculated for the same system as Figs. 2 and 3. The value of C_P is obtained via the fluctuation of the relative entropy ΔS [19], i.e., C_P
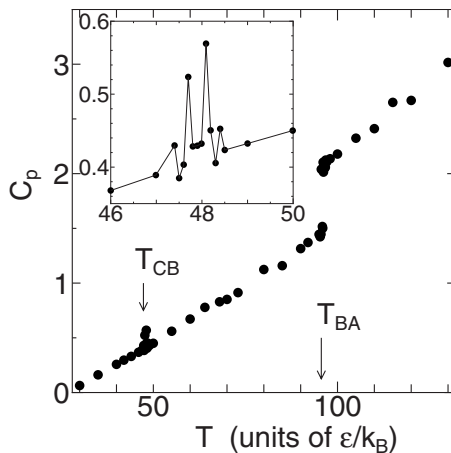

FIG. 5. Molar heat capacity C_P in arbitrary units (obtained from fluctuation of relative entropy) vs temperature T for $N=1344$ parallel soft spherocylinders with $L=2$ at $P=1000$. Inset shows C_P around T_{CB}.
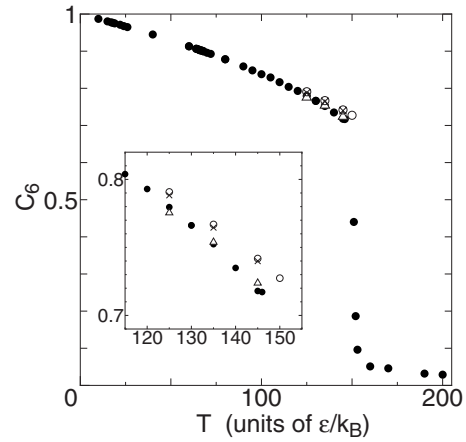

FIG. 6. Sixfold bond orientational order C_6 vs temperature for parallel soft spherocylinders with $L=4$ at $P=1000$. ●, $N=1344$ with six layers; ○, $N=2340$ with three layers; △, $N=4680$ with six layers; ×, $N=9360$ with three layers. Inset shows close-up near Hex$B$-SmA transition.

$\propto (\langle S^2 \rangle - \langle S \rangle^2)$, thus expressed in arbitrary units. In Fig. 5, not only peaks at T_{CB} but also a step in the value at T_{BA} can be discerned. The double peak at T_{CB} may result from fluctuation induced force near the critical point confined in periodic boundary conditions [20]. Anomalous fluctuation at low temperatures, as reported in [21], was also observed in our simulations. To get reasonable values of second-ordered thermodynamic quantities such as C_P required slow relaxation at lower temperatures with weak coupling to the thermostat, especially in the crystal phase ($t \geq 4000$ in simulation time using mass of thermostats kinetic energy $K=20\,000$ [2]). When the system was forced to relax fast by strong coupling to the thermostat (through $K=20$), reasonable average values of first-order thermodynamic quantities were obtained but resulted in larger values of fluctuation which do not decay, thus, not leading to reasonable values of second-order thermodynamic quantities. It has been reported that strong coupling to the thermostat results in cutting off fluctuations of low frequencies [22], which must influence the second-order thermodynamic quantities. These results clearly show that it is important to relax the system with weak coupling to the thermostat to get proper values of second-order thermodynamic quantities.

Figure 6 shows the sixfold bond orientational order parameter

$$C_6 = \left\langle \left| \frac{1}{N_b} \sum_j^N \sum_k \cos(6\theta_{kj}) \right| \right\rangle, \qquad (4)$$

where j runs over all molecules in the system, k runs over all the nearest-neighbor molecules of j, θ_{kj} is the angle between the fixed x axis and the projection of the line connecting the center of mass of particles k and j on the xy plane, and N_b denotes the total number of bonds in the system. The bracket $\langle\ \rangle$ denotes the time average of duration $\Delta t = 10$ (1×10^5 time steps). Note that C_6 contains the information of all layers in the system. The inset shows how the system size affects the value of C_6. It can be seen that the number of layers in the
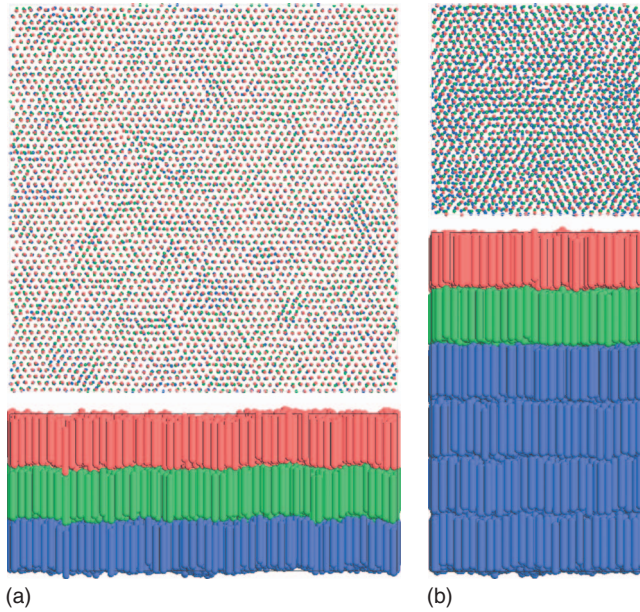
FIG. 7. (Color) Snapshots for systems with $L=4$ at $P=1.0 \times 10^3$ (a) $N=9360$ at $T=135$; (b) $N=4680$ at $T=125$.

FIG. 8. Positions relative from original projected on the xy plane in Hex$B$ phase at (a) $T=73$ for time duration $\Delta t=1000$ and (b) $T=90$ for $\Delta t=500$, for $N=1344$ parallel soft spherocylinders with $L=2$, $M=0.01$, and $K=20\,000$ at $P=1000$.

system affects the value of C_6. The Hex$B$ phase appears for $0.717 \leq C_6 \leq 0.975$ for $L=4$. The values of C_6 at T_{BA} are in the range of $0.65 < C_6 < 0.72$ with smaller values for shorter molecules. The values at T_{CB} are $0.65 < C_6 < 0.98$, reflecting that the values of T_{CB} becoming lower (thus resulting in higher C_6) for systems with longer molecules. In Fig. 7, we show some snapshots in the Hex$B$ phase where the values of C_6 are shown in Fig. 6. In the bird's eye view of these snapshots (upper panel), the molecules are shown small to reveal the relative positions of different layers.

Although the specific volume and C_6 vary continuously at T_{CB}, the dynamics drastically change. At temperatures above T_{CB}, hopping dynamics is observed. In Hex$B$ phase, diffusion of the particles inside each layer (in xy plane) increases as the temperature rises and shows a high value of diffusion at temperatures near T_{BA}. Fluctuations of the layer positions are also observed in the Hex$B$ phase, however, diffusion of molecules among different layers (z direction) only occurs at temperatures much higher than T_{BA}. In Fig. 8, positions of all the molecules (projected on xy plane) relative to that at a certain time are plotted. If the molecule does not move for the period of time, a dot will be plotted on (0,0) for such
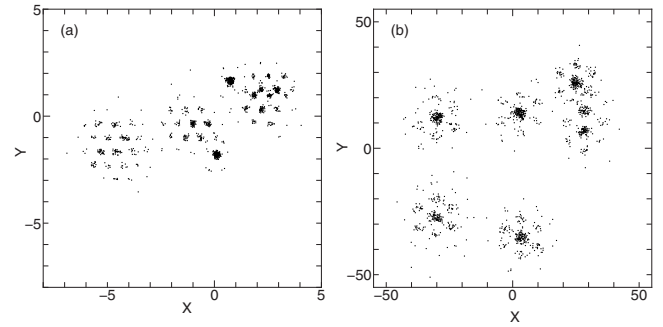
diagrams. In the crystal phase, dots are crowded near (0,0) since molecules only fluctuate around their equilibrium positions. In Hex$B$ phase, hopping to other vacant sites occurs as shown in Fig. 8 and dynamical heterogeneity is clearly observed. There are patches of hexagonal lattice which are out of position with each other. In addition to the molecular hopping, the hexatic patches themselves diffuse in the long run which is the reason for not having many points near (0,0). Since Fig. 8 contains data of all the molecules in six layers, it also shows that correlation between the layers exists. The hopping dynamics in Hex$B$ phase was also observed in Monte Carlo simulations and was used as a criterion to define the boundary between Cry and Hex$B$ phases [9] along with the value of C_6. From our simulation, it is clear that at temperatures close to T_{CB} (identified from relative entropy), the hopping rate is negligibly small and has intermittent characteristics, thus difficult to get reliable statistics even in the longest run. We also have seen in the previous paragraph that the values of C_6 cannot be a reliable quantity either to predict the transition temperatures, especially T_{CB}.

MD simulations have been conducted for a model of liquid crystals and the nature of Cry-Hex$B$-SmA phase transition has been investigated. The transition temperatures were identified by relative entropy and heat capacity. In the Hex$B$ phase, hopping dynamics has been observed. It has been shown that the high-precision symplectic integrator designed for simulating soft matter is effective in investigating not only the dynamics but also the thermodynamics of the system.

[1] D. Frenkel and B. Smit *Understanding Molecular Simulation: From Algorithms to Applications*, 2nd ed. (Academic, London, 2002); H. J. C. Berendsen, *Simulating the Physical World: Hierarchical Modeling from Quantum Mechanics to Fluid Dynamics* (Cambridge University Press, Cambridge, England, 2007); H. Meirovitch, Curr. Opin. Struct. Biol. **17**, 181 (2007).

[2] K. M. Aoki, J. Phys. Soc. Jpn. **77**, 044003 (2008).

[3] C. C. Huang and T. Stoebe, Adv. Phys. **42**, 343 (1993); P.

Oswald and P. Pieranski, *Smectic and Columnar Liquid Crystals* (Taylor & Francis, Boca Raton, FL, 2006).

[4] D. R. Nelson, *Defects and Geometry in Condensed Matter Physics* (Cambridge University Press, Cambridge, England, 2002).

[5] A. Stroobants, H. N. W. Lekkerkerker, and D. Frenkel, Phys. Rev. A **36**, 2929 (1987); D. Frenkel, J. Phys. Chem. **92**, 3280 (1988); J. A. C. Veerman and D. Frenkel, Phys. Rev. A **41**,

3237 (1990); **43**, 4334 (1991); **45**, 5632 (1992); S. C. Mc-Grother, D. C. Williamson, and G. Jackson, J. Chem. Phys. **104**, 6755 (1996); P. Bolhuis and D. Frenkel, *ibid.* **106**, 666 (1997).

[6] K. M. Aoki and T. Akiyama, Mol. Cryst. Liq. Cryst. **262**, 543 (1995); Mol. Simul. **16**, 99 (1996); Mol. Cryst. Liq. Cryst. **299**, 45 (1997); M. S. Al-Barwani and M. P. Allen, Phys. Rev. E **62**, 6706 (2000); D. J. Earl, J. Ilnytskyi, and M. Wilson, Mol. Phys. **99**, 1719 (2001); K. M. Aoki, M. Yoneya, and H. Yokoyama, Mol. Cryst. Liq. Cryst. **366**, 117 (2001); **413**, 109 (2004).

[7] K. M. Aoki and F. Yonezawa, Phys. Rev. Lett. **69**, 2780 (1992).

[8] L. De Gaetani and A. Tani, J. Chem. Phys. **126**, 064909 (2007).

[9] G. Brannigan, A. C. Tamboli, and F. L. H. Brown, J. Chem. Phys. **121**, 3259 (2004).

[10] K. Schmidt-Rohr and H. W. Spiess, Phys. Rev. Lett. **66**, 3020 (1991); A. Heuer, Phys. Rev. E **56**, 730 (1997); S. Sen and J. F. Stebbins, Phys. Rev. Lett. **78**, 3495 (1997).

[11] T. Kihara, Rev. Mod. Phys. **25**, 831 (1953).

[12] J. D. Weeks, D. Chandler, and H. C. Andersen, J. Chem. Phys.

[13] J. M. Sanz-Serna and M. P. Calvo, *Numerical Hamiltonian Problems* (Chapman & Hall, London, 1994).

[14] K. M. Aoki, M. Yoneya, and H. Yokoyama, J. Chem. Phys. **120**, 5576 (2004).

[15] C. P. Dettmann and G. P. Morriss, Phys. Rev. E **55**, 3693 (1997); S. D. Bond, B. J. Leimkuhler, and B. B. Laird, J. Comput. Phys. **151**, 114 (1999); J. Sturgeon and B. B. Laird, J. Chem. Phys. **112**, 3474 (2000); S. Nosé, J. Phys. Soc. Jpn. **70**, 75 (2001).

[16] K. M. Aoki and F. Yonezawa, Phys. Rev. E **48**, 2025 (1993).

[17] H. Qian and J. J. Hopfield, J. Chem. Phys. **105**, 9292 (1996).

[18] G. Poeti, E. Fanelli, and D. Guillon, Mol. Cryst. Liq. Cryst. **82**, 107 (1982).

[19] L. D. Landau and E. M. Lifshitz, *Statistical Physics* (Butterworth-Heinemann, Oxford, 1980).

[20] M. Krech, J. Phys.: Condens. Matter **11**, R391 (1999); A. E. Ferdinand and M. Fisher, Phys. Rev. **185**, 832 (1969).

[21] R. Simonazzi and A. Tenenbaum, Phys. Rev. E **54**, 964 (1996).

[22] B. L. Holian, A. F. Voter, and R. Ravelo, Phys. Rev. E **52**, 2338 (1995).